VOLUME 86, NUMBER 15 PHYSICAL REVIEW LETTERS 9 APRIL 2001

Hamiltonian of the V_{15} Spin System from First-Principles Density-Functional Calculations

Jens Kortus,* C. Stephen Hellberg, and Mark R. Pederson
Center for Computational Materials Science, Code 6390, Naval Research Laboratory, Washington, D.C. 20375

(Received 11 July 2000)

We report first-principles all-electron density-functional-based studies of the electronic structure, magnetic ordering, and anisotropy for the V_{15} molecular magnet. From these calculations, we determine a Heisenberg Hamiltonian with five antiferromagnetic and one *ferromagnetic* exchange couplings. We perform direct diagonalization to determine the temperature dependence of the susceptibility. This Hamiltonian reproduces the experimentally observed spin $S = 1/2$ ground state and low-lying $S = 3/2$ excited state. A small anisotropy term is necessary to account for the temperature independent part of the magnetization curve.

DOI: 10.1103/PhysRevLett.86.3400 PACS numbers: 75.50.Xx, 75.30.Et, 75.30.Gw, 75.45.+j

With the continued interest in the fabrication and optimization of miniaturized magnetic devices [1], future design considerations will require an understanding of nanoscale magnetic systems. In order to transition such materials into simple devices it is necessary to be able to explain how interactions such as spin-spatial coupling and spin-spin exchange effects may couple collectively to create a seemingly single-spin system. Further, it is necessary to determine the temperature range at which such systems will indeed behave collectively. In general the properties of a nanoscale system of coupled spins depend directly on the strength of the exchange parameters and on the size and sign of the anisotropy energy due to spin-orbit coupling. While these parameters are generally determined by the transition metal atoms, the ligands and other nonmagnetic atoms are responsible for stabilizing the array of spins. Requisite to a complete computational understanding of such spin systems is the ability to account for the strong ligand-metal interactions and to determine whether the behavior of a given spin system is mainly mediated by the anisotropy, by spin-spin coupling, or by a combination of the two.

Recently, the Mn_{12}-acetate and Fe_8 molecules [2] have attracted considerable interest because they behave as high-single-spin systems (total spin $S = 10$) at temperature ranges on the order of 20–60 K. Because of their large magnetomolecular anisotropy energy these systems retain their moment orientation at reasonably high temperatures and exhibit the phenomena of resonant tunneling of magnetization at well defined magnetic fields [3,4].

The $K_6[V_{15}As_6O_{42}(H_2O)]8H_2O$ molecular crystal, first synthesized by Müller and Döring [5,6], represents a transition-metal spin system in the same size regime as the Mn_{12} and Fe_8 molecular crystals. In contrast to Mn_{12} and Fe_8 molecules, the V_{15} molecule is thought to behave as a weakly anisotropic magnet composed of 15 spin $s = 1/2$ particles which couple together to form a molecule with a total spin $S = 1/2$ ground state. Besides the fundamental interest in understanding quantum effects in these nanomagnets, they might be also relevant for implementations of quantum computers [7]. Calculations on such correlated systems present a challenge to mean-field frameworks such as density-functional theory because it is often not possible to construct a single collinear reference state which preserves the inherent symmetry of the system and has the correct spin quantum numbers.

This work utilizes an efficient coupled multilevel analysis which relies on fitting density-functional energies to mean-field Heisenberg or Ising energies in order to determine the exchange parameters. The approximate exchange parameters gleaned from the first N Ising configurations were used to find the next lowest energy Ising configuration and subsequently to improve the parametrization of the exchange parameters. "Self-consistency" of this approach is determined when the predicted Ising levels are unchanged by the addition of data from new Ising configurations. The coupling of the density-functional method to a classical Ising representation allowed us to determine the exchange parameters by considering only several spin configurations. Further, the resulting ground-state spin configuration within density-functional theory exhibits the correct spin projection of $1/2$. With the exchange parameters determined, we diagonalize the complete many-body Heisenberg Hamiltonian to calculate the susceptibility and spin correlation functions for comparison with experiment. The many-body basis is complete, so all states are allowed including noncollinear spin arrangements and quantum disordered phases [8].

Starting from x-ray data [9] we generated several unit cells and isolated a single $K_6[V_{15}As_6O_{42}(H_2O)]$ unit. In order to optimize the geometry within the quasi- D_3 symmetry of the V_{15} molecule [5], we initially replaced the statistically oriented water molecule at the center of the molecule by a neon atom and used an $S = 3/2$ spin configuration which does not break the crystallographic symmetry. The Ising configuration of this molecule consists of three aligned spin-$\frac{1}{2}$ V atoms in the triangle and equivalent upper and lower hexagons composed of a ring of antiferromagnetically (AF) coupled spin-$\frac{1}{2}$ V atoms.

The geometry of the molecule was then optimized within the all-electron density-functional methodology using the generalized-gradient approximation (GGA) [10]. The

0031-9007/01/86(15)/3400(4)$15.00

calculations were performed with the Naval Research Laboratory Molecular Orbital Library (NRLMOL) [11]. Calculations on 49 geometrical configurations were performed during the conjugate-gradient relaxation of the molecule. Subsequent calculations show that the geometrical, electronic, and magnetic properties of this system are unaffected by the presence or type of inert moiety enclosed within the void. Using this geometry, we performed eleven additional calculations on different spin configurations (see Table I) to determine the six exchange parameters (J's) of the Heisenberg Hamiltonian

$$H = \sum J_{ij} \mathbf{S}_i \cdot \mathbf{S}_j \,, \tag{1}$$

as well as the spin configuration of the density-functional ground state [8]. The J's used in the above Hamiltonian are defined according to Fig. 1. As shown in Table I, we have included high-spin configurations (XI, XII, XIII), which generally have some symmetry as well as lower-spin nonsymmetric configurations. The energy for the high-spin $S = 15/2$ ferromagnetic (FM) state (XIII) of 873 meV is predominantly caused by a large AF exchange coupling (J) between the most closely bonded hexagonal V atoms. However, the 113 meV splitting between the $S = 9/2$ and $S = 15/2$ states (XII and XIII) shows that there is a reasonably strong AF coupling, approximately 18 meV on average, between the triangular and hexagonal atoms. All of the data displayed in Table I have been used to determine the exchange parameters from a least square fit to the mean-field solution of the Heisenberg Hamiltonian (1). The fit is very good with errors ranging from 0.1–1.55 meV. The fit leads to exchange parameters of $J = 290.3$ meV, $J' = -22.7$ meV, $J'' = 15.9$ meV, $J1 = 13.8$ meV, $J2 = 23.4$ meV, and $J3 = 0.55$ meV, where positive numbers correspond to AF and negative ones to FM interactions. The *ferromagnetic* interaction J' is a surprising result [12] and deserves further discussion since it is qualitatively different from earlier assumptions based on entirely AF interactions [6,13]. Ferromagnetic coupling is possible without polarizing the oxygens through a 4th order process similar to superexchange. In superexchange, the intermediate state has the lowest d orbital on the V doubly occupied with up and down electrons [14]. However, electrons can also hop to higher energy d orbitals on the V's. In this case both parallel and antiparallel spins are allowed without violating the Pauli exclusion principle, but Hund's rule coupling prefers parallel alignment. The superexchange process (same d orbital) completely excludes the process with same-spin electrons while the FM process (different d orbitals) merely favors FM alignment. Thus a FM coupling is obtained if the V-O hopping matrix elements into the higher d orbital are significantly larger than the matrix elements for the hopping of O electrons into the lowest energy d orbital. The occurrence of such interactions is possible in a low-symmetry system such as the one studied here.

Even with this FM interaction, our spin Hamiltonian yields an $S = 1/2$ ground state composed largely of Ising configurations similar to the one depicted in Fig. 1. This Ising configuration was predicted from the J's from earlier fits to DFT energies and corresponds to the ground-state DFT configuration (I).

We have fully diagonalized the Heisenberg Hamiltonian (1). Using all symmetries, the largest irreducible many-body subspace has dimension 2145. We find a spin-$1/2$ Kramer doublet as the ground state with a low-lying spin-$3/2$ quadruplet as shown in Fig. 1. The rest of the spectrum is well separated from these eight states. The large value of J binds the spins in the hexagons into singlets. The low-energy physics arises from the inner triangle spins interacting with each other both directly and with an effective coupling through the hexagons, yielding the doublet-quadruplet spectrum [15]. There are two important energy scales in the spectrum: Δ, the gap between the doublet and quadruplet, and J, the energy at which the

TABLE I. DFT energies (E) of calculated Ising configurations, energies obtained from the fit, and $4\langle S_i^q S_j^q \rangle$ along each of the six bonds. Also included is the anisotropy shift δ for the $M_s = S$ state of each Ising configuration. A least square fit of this data leads to exchange parameters of $J = 290.3$, $J' = -22.7$, $J'' = 15.9$, $J1 = 13.8$, $J2 = 23.4$, and $J3 = 0.55$ meV.

E (meV)	Fit	J	J'	J''	$J1$	$J2$	$J3$	Spin	Label	δ (K)
−78.37	−78.44	−6	2	−2	6	−6	−1	1/2	I	0.8
−73.39	−73.63	−6	2	−2	4	−4	−1	1/2	II	
−35.48	−35.08	−6	−2	2	4	−4	−1	1/2	III	
−34.89	−34.53	−6	−2	2	4	−4	3	3/2	IV	
0.00	−0.79	−6	−6	6	6	−6	3	3/2	V	1.5
8.38	8.28	−6	−6	6	2	−2	−1	1/2	VI	1.3
28.14	28.08	−6	−6	6	−6	6	3	3/2	VII	
126.32	126.14	−4	−4	6	4	−6	3	1/2	VIII	
129.17	128.88	−4	−4	2	6	−4	3	5/2	IX	
278.35	278.50	−2	−6	2	4	−4	3	3/2	X	
434.22	435.78	0	0	6	6	0	3	9/2	XI	1.6
760.75	760.76	6	6	6	−6	−6	3	9/2	XII	1.6
873.11	872.35	6	6	6	6	6	3	15/2	XIII	1.8

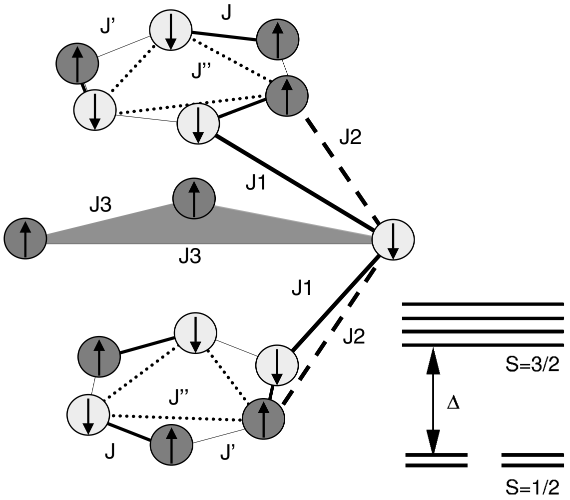

FIG. 1. The 15 magnetic vanadium atoms of the $K_6[V_{15}As_6O_{42}(H_2O)]$ molecule. They form two hexagonal layers and an inner triangular layer of vanadium atoms sandwiched within. The arrows show the lowest energy spin configuration found from DFT calculations. The six exchange parameters used in the Heisenberg Hamiltonian are shown as lines. Schematically displayed are energy levels of the Kramer doublet ($S = 1/2$) ground state and the low-lying quadruplet ($S = 3/2$) separated by Δ.

singlets in the hexagon break and the molecule starts to behave as more than three spins.

The low-energy effective interaction between inner triangle spins proceeds via $J1$ and $J2$ (which frustrate each other) to a hexagon singlet, via J' and J'' to a neighboring singlet, and finally via $J1$ and $J2$. A larger contribution to Δ comes from a direct interaction through $J3$ mediated by hopping through O and As levels. Thus simple perturbation theory [6] yields

$$\Delta = \frac{3}{4}\frac{(J2 - J1)^2(J'' - J')}{J^2} + \frac{3}{2}J3\,. \qquad (2)$$

Comparing our calculated susceptibility with experiment [13], we find the low-temperature behavior indicates our doublet-quadruplet gap $\Delta \approx 10$ K to be significantly larger than the experimental value of $\Delta \approx 3.7$ K, while the high-temperature behavior shows our calculated value of J is too large. Both of these discrepancies can be explained almost entirely by J's that are too large within the density-functional-based treatment, as known for other vanadium systems [8].

Agreement with experiment for the low temperature Δ can be achieved by dividing all J's by a constant factor of 2.9. Figure 2 shows our calculated result with rescaled J's compared to experimental data from Chiorescu. A uniform scaling of our calculated exchange parameters is not able to obtain the right low and high temperature behavior at the same time. The high temperature behavior could be improved by further reducing J with corresponding adjustments to the other couplings to keep Δ constant.

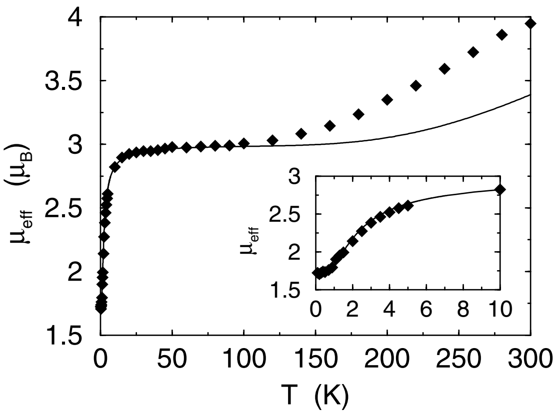

FIG. 2. The effective moment $\mu_{\rm eff} = \sqrt{3\chi T}$ calculated with all J's uniformly rescaled by dividing by a constant factor of 2.9. The diamonds are the actual experimental values from Chiorescu. The inset shows the low temperature behavior.

A set of AF interactions [6] also fits the experimental results. In fact any set of parameters with the correct values of J and Δ given by Eq. (2) will fit the effective moment well. To support future efforts aimed at experimentally confirming our relative parameters, we have calculated the spin-spin correlation function $C_S = 4\langle S_i^q \cdot S_j^q \rangle$, with q representing the arbitrary quantization axis. Since J is always largest, the spins tend to form a singlet along this bond, yielding $C_S(J) \cong -1$ (AF correlation). The three inner triangle spins form a noncollinear arrangement with $C_S \cong -0.33$ between all pairs of spins. The direct $J3$ coupling reduces the correlations between triangle and hexagon spins. We find $C_S(J1) \cong +0.02$ and $C_S(J2) \cong -0.02$ (FM and AF correlations, respectively), while the coupling constants of Ref. [6] yield $C_S(J1) \cong +0.12$ and $C_S(J2) \cong -0.14$. This prediction should be measurable with neutron scattering.

Chiorescu *et al.* observe that rotation of the spin projection is achieved without encountering a barrier [13] and Dobrovitski *et al.* posit that the V_{15} molecule is indeed a low anisotropy system [15]. As shown below the existence of either easy-plane or easy-axis anisotropy will shift the $M_s = 3/2$–$1/2$ Zener-Landau tunneling transitions that have been observed by Chiorescu *et al.* [13].

Recently, Pederson and Khanna have developed a new method for accounting for second-order anisotropy energies [16]. This method relies on a simple albeit exact method for spin-orbit coupling and a second-order perturbative treatment of the spin-orbit operator to determine the dependence of the total energy on spin projection. Initial applications to Mn_{12} lead to a density-functional-based second-order anisotropy energy of 55.7 K [17] which is in essential agreement with the experimentally deduced values of 55.6 K [18]. We have generalized this methodology to systems with arbitrary symmetry and have calculated the anisotropy energy for several different spin configurations of the V_{15} molecule.

We have calculated the anisotropy energy for the lowest Ising configurations with one, three, nine, and fifteen unpaired electrons, as given in Table I. In all cases we find that the V_{15} possesses weak easy-plane anisotropy. This result ensures that anisotropy effects will not change the total spin of the V_{15} ground state. Examination of the expression for the second order anisotropy energy in Ref. [16], shows that such energies do not necessarily scale as the square of the total moment. Indeed, as shown in Table I, we find that the anisotropic effects are in fact only weakly dependent on the total spin and that the energy of the $M_s = S$ state increases by approximately $\delta = 0.8$ to 1.8 K. Chiorescu *et al.* show that the broadening of the Zener-Landau tunneling fields decreases with temperature for the $|1/2, 1/2\rangle$ to $|1/2, -1/2\rangle$ transitions but are independent of temperature for the $|3/2, 3/2\rangle$ to the $|3/2, 1/2\rangle$ transitions [13]. This behavior is exactly what is expected from a sample containing weak easy-plane spin anisotropy. At sufficiently low temperatures, only the $S = 3/2$ and $S = 1/2$ states are relevant, and the field-dependent crossing of these states depends on whether the magnetic field is parallel or perpendicular to the easy plane. The broadening is proportional to the difference of the magnetic anisotropy energy for the different spin configurations involved. Because of the small anisotropy in V_{15} the effect will be small. Although it is not possible to translate the DFT obtained anisotropy energies directly to the quantum mechanical many-spin ground state discussed here, we obtain from these energies tunnel field broadenings between 0.1 to 0.48 T which envelop the experimentally observed field broadening of about 0.2 T [13]. In powdered samples, the small easy-plane anisotropy would lead to a broadening in the tunneling field and in single crystals the effect would change the tunneling fields as a function of field orientations.

To summarize, we have performed accurate all-electron density-functional calculations on the V_{15} cluster as a function of geometry and spin configuration. By dynamically coupling the mean-field density-functional approach to exact-diagonalization of a many-spin Heisenberg representation, we have efficiently determined the lowest density-functional configurations and the entire Heisenberg spin excitation spectrum. Our calculations suggest that the small experimentally observed orientational dependence of the tunneling field for the $M_s = 3/2$ to $M_s = 1/2$ is a signature of configuration dependent magnetic anisotropy in this molecule. The method used here is general and allows one to characterize both systems which are potentially useful for magnetic storage (Mn_{12}, Fe_8) and systems which show quantum coherence, such as the one studied here.

This work was supported in part by ONR Grants No. N0001498WX20709 and No. N0001400AF00002. Computations were performed at the DoD Major Shared Resource Centers. We thank I. Chiorescu for enlightening discussions and for supplying the data used in Fig. 2.

---

*Present address: MPI für Festkörperforschung, Postfach 80065, D-70506 Stuttgart, Germany.

[1] R.F. Service, Science **287**, 1902 (2000); S. Sun, C.B. Murray, D. Weller, L. Folks, and A. Moser, Science **287**, 1989 (2000).
[2] A. Caneschi, D. Gatteschi, C. Sangregorio, R. Sessoli, L. Sorace, A. Cornia, M.A. Noval, C. Paulsen, and W. Wernsdorfer, J. Magn. Magn. Mater. **200**, 182 (1999), and references there.
[3] J. Friedman, M.P. Sarachik, J. Tejada, and R. Ziolo, Phys. Rev. Lett. **76**, 3820 (1996); L. Thomas, F. Lionti, R. Ballou, D. Gatteschi, R. Sessoli, and B. Barbara, Nature (London) **383**, 145 (1996).
[4] C. Sangregorio, T. Ohm, C. Paulsen, R. Sessoli, and D. Gatteschi, Phys. Rev. Lett. **78**, 4645 (1997).
[5] A. Müller and J. Döring, Angew. Chem., Int. Ed. Engl. **27**, 1721 (1988).
[6] D. Gatteschi, L. Pardi, A.L. Barra, A. Müller, and J. Döring, Nature (London) **354**, 463 (1991).
[7] N.D. Mermin, Phys. Today **53**, No. 7, 11 (2000); D.P. DiVincenzo and D. Loss, J. Magn. Magn. Mater. **200**, 202 (1999).
[8] C.S. Hellberg, W.E. Pickett, L.L. Boyer, H.T. Stokes, and M.J. Mehl, J. Phys. Soc. Jpn. **68**, 3489 (1999).
[9] A. Müller and J. Döring, Z. Anorg. Allg. Chem. **595**, 251 (1991).
[10] J.P. Perdew, K. Burke, and M. Ernzerhof, Phys. Rev. Lett. **77**, 3865 (1996).
[11] M.R. Pederson and K.A. Jackson, Phys. Rev. B **41**, 7453 (1990); K.A. Jackson and M.R. Pederson, Phys. Rev. B **42**, 3276 (1990).
[12] M.A. Korotin, I.S. Elfimov, V.I. Anisimov, M. Troyer, and D.I. Khomskii, Phys. Rev. Lett. **83**, 1387 (1999).
[13] I. Chiorescu, W. Wernsdorfer, A. Müller, H. Bögge, and B. Barbara, Phys. Rev. Lett. **84**, 3454 (2000); cond-mat/9911180.
[14] J.B. Goodenough, *Magnetism and the Chemical Bond* (Wiley, New York, 1963).
[15] V.V. Dobrovitski, M.I. Katsnelson, and B.N. Harmon, Phys. Rev. Lett. **84**, 3458 (2000).
[16] M.R. Pederson and S.N. Khanna, Phys. Rev. B **60**, 9566 (1999).
[17] M.R. Pederson and S.N. Khanna, Chem. Phys. Lett. **307**, 253 (1999); M.R. Pederson and S.N. Khanna, Phys. Rev. B **59**, R693 (1999).
[18] A.L. Barra, D. Gatteschi, and R. Sessoli, Phys. Rev. B **56**, 8192 (1997).